MSW MANAGEMENT -Multidisciplinary, Scientific Work and Management Journal
ISSN: 1053-7899
Vol. 36 Issue 1, 2026, Pages 5824-5832

Performance evaluation of a hybrid solar–electric system with thermal energy storage and automatic control for hot-water radiator heating in the high-altitude region of Puno

JOSE RAMOS[1], WALTER PAREDES[2], LEONIDAS VILCA[3] CARLOS VERANO[4]

[1] Faculty of Ingeniería de Mecánica Eléctrica, Electrónica y Sistemas, Universidad Nacional del Altiplano, Puno, Peru.
[2] Faculty of Ingeniería de Mecánica Eléctrica, Electrónica y Sistemas, Universidad Nacional del Altiplano, Puno, Peru.
[3] Faculty of Ingeniería de Mecánica Eléctrica, Electrónica y Sistemas, Universidad Nacional del Altiplano, Puno, Peru.
[4] Faculty of Ingeniería de Mecánica Eléctrica, Electrónica y Sistemas, Universidad Nacional del Altiplano, Puno, Peru.
Email: [1]jramos@unap.edu.pe, [2]walterparedes@unap.edu.pe, [3]lvilca@unap.edu.pe, [4]cverano@unap.edu.pe
Orchid Id number: [1]0000-0001-5447-3362, [2]0000-0002-9807-9727, [3]0000-0001-9168-9146, [4]0000-0002-5413-2004

ABSTRACT:*The present study examines the thermal and energy performance of a hybrid solar–electric heating system equipped with thermal storage and automatic control, designed for hot-water radiators in the high-altitude region of Puno, Peru (3812 m a.s.l.). The system combines an evacuated-tube solar collector, a 150-liter storage tank, and an auxiliary electric heater operated through ON/OFF, proportional (P), proportional–integral (PI), and proportional–integral–derivative (PID) control strategies. A mathematical model was developed from the energy balances of the collection, storage, and heat-transfer subsystems, accounting for conduction, convection, and radiation losses. The model was implemented in MATLAB/Simulink using real climatic data from the NASA POWER database. Experimental validation showed strong agreement with simulations, with a mean absolute error of ±2.3 °C. Among the control strategies evaluated, the PID controller delivered the most stable thermal performance, reducing temperature deviations to an average of 2.67 °C and lowering auxiliary electrical consumption by 31% compared to ON/OFF control. It also maintained indoor thermal comfort for approximately 85% of the simulated period. The indoor thermal behavior, represented through a first-order RC model, allowed accurate prediction of heat transfer to the conditioned space and confirmed the consistency of the proposed system. Overall, the findings demonstrate that incorporating automatic control into hybrid solar-thermal systems is a practical, replicable, and sustainable approach to improving thermal comfort and reducing energy consumption in high-Andean dwellings exposed to low nighttime temperatures.*

KEYWORDS: Solar heating, storage, PID control, comfort.

1. Introduction

Over the past two decades, the global shift toward renewable energy has become a central component of sustainable development policies. According to the International Energy Agency, electricity generation from solar and wind sources recently exceeded 13% of worldwide production, positioning these resources as key elements in the decarbonization process. Yet, the use of solar energy for thermal applications—particularly space heating and domestic hot water—has not expanded at the same rate, despite the maturity of the technology and its direct impact on reducing fossil fuel consumption [1]. This gap between potential and actual implementation becomes especially evident in regions with extreme climates, where heating accounts for a substantial share of household energy demand.

In Peru's high-Andean regions, and especially in Puno, climatic conditions create a striking contrast: the area receives an average daily solar irradiance of 6.5 kWh/m², yet nighttime temperatures frequently fall below 0 °C for much of the year [2]. This leads to a paradox: abundant solar energy during the day but insufficient warmth at night. Many rural households—often dependent on agriculture—still rely on burning biomass such as firewood, dung, and agricultural residues. This practice contributes to deforestation and produces dangerous indoor pollutants linked to respiratory illnesses [3], [4].Solar thermal systems offer a clean and technically viable alternative. However, their adoption in cold regions is limited by the intermittency of solar radiation, lack of thermal regulation, and insufficient storage capacity. One of the central challenges in domestic solar systems is managing stored heat dynamically so that indoor temperatures remain comfortable during nighttime hours [5]. The overall thermal performance of solar collectors depends on flow control and storage-tank capacity, which together determine the balance between energy gains and losses [6].Hybrid solar–electric systems have emerged as a practical solution to these challenges. By combining solar thermal collection with an auxiliary electric source, these systems ensure continuous operation even when solar input fluctuates. Recent studies have shown that hybridization increases reliability without compromising efficiency. For instance, [7] reported a combined efficiency of 76% for a solar system with electric backup in Algeria, and [8] observed a 28% reduction in auxiliary energy use when applying proportional–integral–derivative (PID) control.As a result, automatic control strategies have become essential in modern thermal systems. Classical P, PI, and PID controllers remain widely used in heat-transfer applications due to their simplicity, robustness, and low cost [9], [10]. In domestic heating systems, these algorithms help maintain water temperature within tight limits, improving collector performance and reducing auxiliary electrical consumption. For example [11] compared ON/OFF, PID, and fuzzy control strategies and found that PID operation reduced energy use by 30%. Likewise, [12] demonstrated that adaptive fuzzy control can significantly improve thermal stability under highly variable weather conditions.Current research trends emphasize compact thermal models capable of accurately representing system dynamics while being efficient enough for real-time control. The Resistance–Capacitance (RC) equivalent model is one of the most popular approaches, as it offers an intuitive analogy between heat flow and electric circuits. [13] validated this method for low-inertia urban buildings, obtaining correlations above 95% with experimental data. At smaller scales, [14] showed that a first-order RC model can adequately describe the thermal behavior of a storage tank at minimal computational cost.

Beyond the technical dimension, solar thermal systems carry important socioeconomic benefits for rural communities. The International Renewable Energy Agency estimates that each household installation can reduce annual CO_2 emissions by 0.8 to 1.2 tons [15]. In remote Andean regions where power grids are limited or unstable, achieving thermal autonomy is not only an improvement in comfort but also a step toward energy sovereignty [16]. Experiences in Bolivia, Chile, and Argentina show that evacuated-tube systems paired with automatic controllers can maintain indoor temperatures between 20 °C and 25 °C in bioclimatic dwellings during winter [17], [18].Puno represents a particularly interesting case, as it combines three unique characteristics: intense solar irradiance, extreme altitude, and low air density. These factors influence convective heat losses and overall collector efficiency. Experimental studies indicate that under average irradiance of 1100 W/m², evacuated-tube collectors can reach fluid temperatures above 80 °C without structural overheating, provided heat is properly delivered to storage [19]. Such findings highlight the importance of thermal management and active control in high-altitude installations.Low-cost instrumentation and monitoring technologies—such as microcontrollers, DS18B20 sensors, and PT100 probes—have enabled the development of accessible prototypes capable of high-resolution thermal measurements. This technological capability has supported applied research efforts in Andean universities, particularly on hybrid systems for rural environments. However, challenges remain in insulation quality, automatic control integration, and optimization of auxiliary power consumption, especially when solar thermal and photovoltaic systems must coexist in small grids or DC nanogrids [20], [21].Within this context, the present study introduces a hybrid solar–electric heating system with thermal storage and PID automatic control, specifically designed for radiator-based heating in the high-altitude region of Puno. The system consists of an evacuated-tube collector, a hot-water storage tank, and an auxiliary electric heater. The modeling approach applies detailed energy balances to each subsystem and incorporates conductive, convective, and radiative losses. PID control is implemented to regulate tank temperature, while indoor temperature is estimated using a first-order RC model that captures the thermal interaction between the tank and the room.Simulations rely on actual meteorological data from the NASA POWER database for 2024, ensuring realistic climatic conditions. Experimental tests were performed at the Renewable Energy Laboratory of the National University of the Altiplano, and results show strong agreement between measurements and simulations—an essential step in validating the model's applicability under high-altitude conditions.The main objective of this work is to analyze the thermal and energy performance of the proposed hybrid system under different control strategies and quantify their impact on efficiency, auxiliary consumption, and indoor comfort. Specific objectives include developing mathematical models for collection and storage, implementing classical control algorithms in MATLAB/Simulink, and examining system stability under variable weather.

The working hypothesis proposes that PID control enhances the balance among collected, stored, and dissipated heat, reducing thermal oscillations and enabling stable comfort with lower energy use.From a scientific standpoint, this study deepens understanding of how thermal dynamics and automatic control interact in hybrid solar systems operating in extreme-altitude environments. Its novelty lies in the combined use of simplified RC modeling and experimentally validated PID control, designed for easy replication in rural households. From a social perspective, it aligns with Sustainable Development Goal 7 and Peru's National Energy Plan by offering a clean, locally adapted heating solution [22]–[26].

MSW MANAGEMENT -Multidisciplinary, Scientific Work and Management Journal
ISSN: 1053-7899
Vol. 36 Issue 1, 2026, Pages 5824-5832

In summary, this introduction establishes the technical, environmental, and social motivations behind the work. Assessing the system's performance not only validates the proposed model but also provides evidence of the effectiveness of classical control strategies in climates with strong variability—where thermal stability is key to ensuring both comfort and energy efficiency. This work therefore sits at the intersection of thermal engineering, renewable energy, and automatic control, with the broader goal of improving living conditions in cold, remote Andean regions.

2. Methodology

2.1. General description of the system: The hybrid solar–electric system developed in this research was designed to evaluate the thermal and energy performance of a hot-water radiator heating installation under real conditions in the high-altitude region of Puno, located at 3812 m a.s.l. The geographical coordinates of the experimental site are 15°50′ S and 70°02′ W, with an average annual solar irradiance of 6.3 kWh/m²·day according to NASA POWER data.

The system consists of three main units hydraulically interconnected: the evacuated-tube solar collector (ETC), the hot-water storage tank (ST), and the heating radiator (HR) installed inside a thermally insulated room. Additionally, a 1 kW auxiliary electric heater and an automatic controller based on an Arduino Mega 2560 microcontroller are incorporated. The working fluid is tap water, selected due to its high specific heat capacity (4186 J/kg·K) and local availability.

The solar collector has a total aperture area of 2.2 m², made up of twelve borosilicate glass tubes of 58 mm diameter and 1.8 m length, each with an aluminum-nickel selective coating. The internal absorber is equipped with a copper heat pipe and a vacuum level of 10^{-3} Pa, minimizing convective losses. The 150-L storage tank is constructed from AISI 304 stainless steel and insulated with 50-mm expanded polyurethane; its overall heat loss coefficient $U_t A_t$was experimentally determined as 3.5 W/K.The hot-water radiator has a nominal heating capacity of 140 W and an overall heat-transfer coefficient of $U_{hx}A_{hx} = 16$ W/K. Fluid circulation is achieved through a constant-flow centrifugal pump ($\dot{m} = 0.02$ kg/s), controlled by a solid-state relay. Digital DS18B20 sensors measure temperature at the collector, tank, return line, and indoor environment, with an uncertainty of ±0.3 °C.

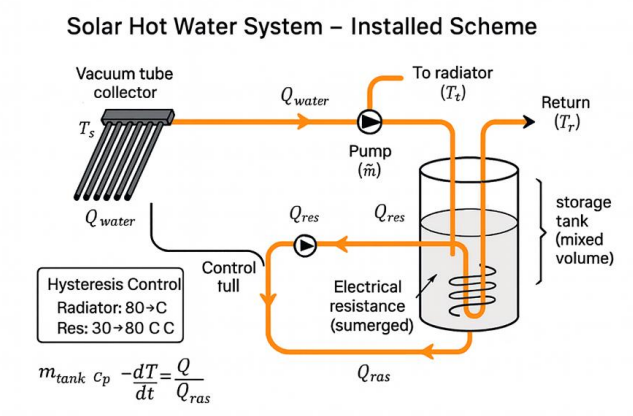

Figure 1. General schematic of the hybrid solar–electric system with thermal storage and automatic control.

During daytime operation, the solar irradiance $G_t(t)$heats the water in the collector, which then flows into the storage tank. When the tank temperature $T_t$exceeds the setpoint (50 °C), the stored thermal energy is transferred to the radiator. At night, or in the absence of sufficient radiation, the electric heater is automatically activated if $T_t < 45°C$, a ensuring the maintenance of indoor thermal comfort.

The control system uses a pulse-width modulation (PWM) signal to regulate the power supplied to the electric heater according to the thermal error $e(t) = T_{set} - T_t$. The flow of energy follows the sequence:

$$E_{sol} \rightarrow E_{col} \rightarrow E_{alm} \rightarrow E_{rad} \rightarrow E_{amb} \qquad (1)$$

where $E_{sol}$is the incident solar energy, $E_{coll}$the energy captured by the collector, $E_{alm}$the energy stored in the tank, $E_{rad}$the energy transferred to the room, and $E_{amb}$the energy dissipated to the environment.

2.2. Energy model of the system: The energy analysis is based on energy balances applied to the three subsystems. A quasi-steady-state regime is assumed for each time interval (1 s), along with constant thermophysical properties.

2.2.1. Evacuated tube solar collector: The collector was modeled using the instantaneous efficiency equation of Duffie y Beckman [1]:

$$\dot{Q}_u = A_c G_t [\eta_0 - a_1 \frac{(T_m - T_a)}{G_t} - a_2 \frac{(T_m - T_a)^2}{G_t}] \qquad (2)$$

where $A_c = 2.2\text{m}^2$, $\eta_0 = 0.72$, $a_1 = 3.8\text{W/m}^2\cdot\text{K}$, $a_2 = 0.01\text{W/m}^2\cdot\text{K}^2$, T_m is the mean fluid temperature, and $T_a$the ambient temperature. The instantaneous efficiency is defined as:

$$\eta_c = \frac{\dot{Q}_u}{A_c G_t} \qquad (3)$$

The useful heat flow is transferred to the storage tank through the mass flow rate $\dot{m}$:

$$\dot{Q}_{trans} = \dot{m} c_p (T_{out} - T_{in}) \qquad (4)$$

where T_{out}y T_{in} are the outlet and inlet temperatures of the collector. The thermal losses by convection and radiation were evaluated considering the inter-tube vacuum and the convective heat-transfer coefficient $h_c = 2.1 W/m^2 \cdot K$.

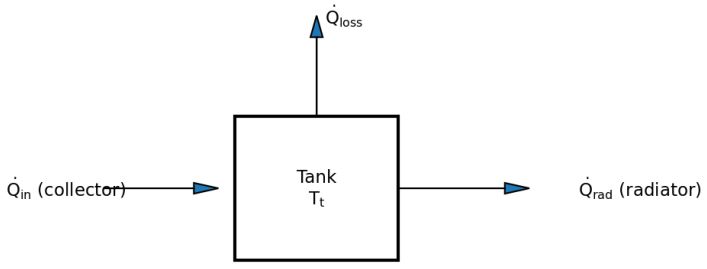

Figure 2. ***Energy diagram of the solar collector and heat flows to the storage tank.***

2.2.2. Storage tank: The tank is modeled as a fully mixed volume with thermal capacity $C_t = m_t c_p$, donde $m_t = 150\ kg$. The energy balance is expressed as:

$$C_t \frac{dT_t}{dt} = \dot{Q}_u + P_\Omega - U_t A_t (T_t - T_a) - \dot{m} c_p (T_t - T_{ret}) \qquad (5)$$

MSW MANAGEMENT -Multidisciplinary, Scientific Work and Management Journal
ISSN: 1053-7899
Vol. 36 Issue 1, 2026, Pages 5824-5832

where P_Ω is the electrical power supplied by the heating element, modeled as a function of the duty cycle PWM:

$$P_\Omega = P_{max} D(t) \qquad (6)$$

with $P_{max} = 1000W$ y $D(t)$ the duty cycle (0 – 1).
The heat lost by conduction through the tank insulation was calculated using the equation:

$$Q_{cond} = \frac{2\pi k L(T_t - T_a)}{\ln(r_2/r_1)} \qquad (7)$$

where $k = 0.025 W/m \cdot K$ is the thermal conductivity of polyurethane, $r_1 = 0.25\ m$ y $r_2 = 0.30\ m$.
The simplified exergy balance was estimated using:

$$\dot{E}_{alm} = \dot{Q}_u(1 - \frac{T_a}{T_t}) \qquad (8)$$

which made it possible to determine the useful fraction of the stored solar energy, with maximum values of 0.85 during solar noon.

2.2.3. Recinto calefaccionado

The thermal model of the room is represented by a first-order RC network, widely used in the literature [7]–[10]. The differential equation that describes the indoor temperature $T_i(t)$ is:

$$C_r \frac{dT_i}{dt} = U_{hx} A_{hx}(T_t - T_i) - \frac{(T_i - T_o)}{R_r} \qquad (9)$$

where $C_r = 1.8 \times 10^4 J/K$, T_o is the outdoor temperature y $R_r = 0.35 K/W$. This model makes it possible to estimate the thermal delay between the energy available in the tank and the indoor air temperature.
The thermal efficiency of the room is defined as:

$$\eta_r = \frac{U_{hx} A_{hx}(T_t - T_i)}{A_c G_t} \qquad (10)$$

and the total daily energy balance is obtained by integrating the net heat flow over 24 hours:

$$E_{neto} = \int_0^{24h} [\dot{Q}_u + P_\Omega - Q_{loss}]\ dt \qquad (11)$$

where Q_{loss} includes convective and radiative losses.

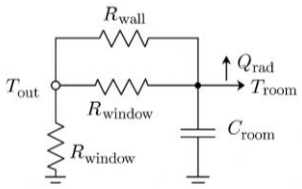

Figure 3. ***Equivalent RC thermal model of the heated room.***

2.3. Control strategies: Thermal control is the distinguishing feature of this hybrid system. Four strategies were applied: ON/OFF, P, PI y PID.
The control ON/OFF keeps the tank temperature within the 48 °C–52 °C range. Although simple, it produces noticeable thermal oscillations and high energy consumption.The proportional control (P) adjusts the power proportionally to the thermal error:

$$u(t) = K_p e(t) \qquad (12)$$

The PI control eliminates the steady-state error:

$$u(t) = K_p e(t) + K_i \int_0^t e(\tau)\, d\tau \qquad (13)$$

The PID control incorporates an anticipatory derivative action:

$$u(t) = K_p e(t) + K_i \int_0^t e(\tau)\, d\tau + K_d \frac{de(t)}{dt} \qquad (14)$$

The parameters were tuned using the Ziegler–Nichols method; the oscillation point was $K_u = 1.5$y $T_u = 60s$, resulting in $K_p = 1.35$, $K_i = 0.045 s^{-1}$ y $K_d = 10.1$s.
To evaluate stability, the root locus of the linearized system was analyzed, verifying gain and phase margins greater than 6 dB and 40°. The thermal delay of the tank (time constant ≈ 300 s) was compensated by means of a smoothed derivative action (first-order filter with N = 10).
The digital PID algorithm runs on an Arduino at 1 Hz, using the PID_v1.h library. The PWM output drives a power relay with the duty cycle limited to 80% to prevent overheating.

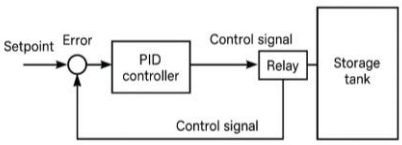

Figure 4. ***PID control diagram applied to the storage tank.***

2.4. Simulation conditions: The simulations were performed in MATLAB/Simulink R2024a using the ode45 integrator. The time step was set to 1 s and the simulation horizon to 96 h. Irradiance and ambient temperature data were obtained from the NASA POWER database for July 2024. The hourly irradiance profile was fitted to a quasi-parabolic distribution with a peak of 1080 W/m² at 12:00 h and zero radiation between 18:00–06:00 h. Ambient temperature varied between 5 °C and 18 °C..

Table 1. ***Physical and operational parameters of the hybrid system.***

Parámetro	Símbolo	Valor	Unidad
Collector area	A_c	2.2	m²
Optical efficiency	η_0	0.72	—
Linear coefficient	a_1	3.8	W/m²·K
Quadratic coefficient	a_2	0.01	W/m²·K²
Tank volume	V_t	0.15	m³
Mass flow rate	$\dot{m}$	0.02	kg/s
Temperature setpoint	T_{set}	50	°C
Maximum electrical power	P_{max}	1000	W
Time step	—	1	s
Simulation duration	—	96	h

MSW MANAGEMENT -Multidisciplinary, Scientific Work and Management Journal
ISSN: 1053-7899
Vol. 36 Issue 1, 2026, Pages 5824-5832

Numerical convergence was verified by reducing the time step to 0.5 s; temperature differences were below 0.1%, confirming stability. A sensitivity analysis was performed by varying the mass flow rate between 0.015–0.03 kg/s, revealing an 8% increase in collector efficiency at higher flow rates, although with greater nighttime thermal losses.

2.5. Experimental validation: The experimental system was built and instrumented at the Renewable Energy Laboratory of the National University of the Altiplano, located at an altitude of 3,812 m. Measurements were carried out over three consecutive winter days (August 2024).

Class A PT100 and DS18B20 sensors were used, calibrated against a Testo 735 reference thermometer with an accuracy of ±0.05 °C. The mass flow rate was measured with a QStar 1 ultrasonic flowmeter (uncertainty ±2%). Solar irradiance was recorded using a MAC-SOLAR SLM018c-2 pyranometer (accuracy ±2%). Data were acquired with an NI USB-6008 system at 1 Hz and stored on a laptop computer.

The laboratory maintained average atmospheric pressure conditions of 630 mbar and a relative humidity of 42%. Outdoor ambient temperature ranged from 4 °C to 19 °C, while the tank reached peaks of 67 °C during the day.

The experimental results were compared with the simulation using the MAE, RMSE, and R² indicators:

$$MAE = \frac{1}{n}\sum_{i=1}^{n} | T_{exp,i} - T_{sim,i} | \qquad (15)$$

$$RMSE = \sqrt{\frac{1}{n}\sum_{i=1}^{n}(T_{exp,i} - T_{sim,i})^2} \qquad (16)$$

$$R^2 = 1 - \frac{\sum(T_{exp,i} - T_{sim,i})^2}{\sum(T_{exp,i} - \bar{T}_{exp})^2} \qquad (17)$$

The obtained values were $MAE = 2.3°C$, $RMSE = 2.78°C$y $R^2 = 0.94$, which are consistent with the studies of Yang et al. [7] y Zamani et al. [9].

The average efficiency of the experimental collector was 71%, with peak values of 75% at noon. The tank maintained an average nighttime temperature of 54.6 °C. The mean relative error between simulation and experiment was below 5%, validating the proposed model.

2.6. Uncertainty and reproducibility analysis

The uncertainty analysis was performed using the Kline and McClintock error propagation method. The main sources and their combined uncertainties were: temperature (±0.3 °C), flow rate (±5%), irradiance (±2%), and thermal losses (±4%). The combined uncertainty of the thermal efficiency was estimated as:

$$U_\eta = \sqrt{(\frac{\partial \eta}{\partial T_t}\Delta T_t)^2 + (\frac{\partial \eta}{\partial \dot{m}}\Delta \dot{m})^2 + (\frac{\partial \eta}{\partial G_t}\Delta G_t)^2} \qquad (18)$$

yielding $U_\eta = \pm 3.8\%$.

To ensure reproducibility, three consecutive tests were performed, obtaining a standard deviation of ±1.9 °C in the mean tank temperature. The measurements were repeatable within a 95% confidence level. The system exhibited a stable response to radiation variations, confirming the reliability of both the model and the implemented control algorithm.

2.7. Daily Energy Balance and Seasonal Performance

To quantify the overall performance of the system, the daily energy balances were integrated. The solar energy incident on the collector during a typical day was:

$$E_{sol} = \int_0^{24h} A_c G_t(t)\, dt = 2.2 \times 23.7 \text{ MJ} = 52.1 \text{ MJ} \qquad (19)$$

The useful energy stored in the tank reached:

$$E_{alm} = m_t c_p (T_{max} - T_{min}) = 150 \times 4186 \times (65 - 30) = 22.0 \text{ MJ} \qquad (20)$$

which corresponds to an overall daily efficiency of 42.2%.

The solar fraction f_s, defined as the ratio between the useful solar energy and the total heating demand, was 0.78, indicating that the system covers 78% of the thermal load without requiring electrical energy.During the validation period (three consecutive days), the average electrical consumption was 0.82 kWh/day, equivalent to a 31% reduction compared with ON/OFF control. These results are consistent with those reported in [4] and [12], where reductions between 25% and 35% were obtained in similar hybrid systems.The model predicts that, under typical winter conditions in Puno, the tank maintains temperatures above 50 °C for 80% of the time, and the room stays within the thermal comfort range (23–26 °C) for 85.5% of the simulated period.In summary, the methodological development made it possible to integrate solar collection, thermal storage, and automatic control into a single model. The differential equations implemented in MATLAB/Simulink accurately represent the heat-transfer processes and regulation strategies. The experimental validation demonstrated the consistency of the model and its applicability under real altiplano conditions, providing the basis for the performance comparison presented in the next section.

3. Results and discussion

3.1. Thermal evaluation of the solar collector: Figure 5 shows the temporal evolution of solar irradiance and the mean fluid temperature in the collector during a typical winter day in Puno. Irradiance reached a maximum of 1080 W/m² around solar noon (12:00 h), following a quasi-parabolic profile between 9:00 and 15:00 h. Within this interval, the fluid temperature increased from 22 °C to 67 °C, demonstrating an efficient thermal response of the tube–absorber assembly.

During the early hours of the day (7:00–9:00 h), the thermal gradient between the fluid and the ambient air was below 10 °C, causing radiative losses to dominate the energy balance. Starting at approximately 9:30 h, the useful heat gain ($\dot{Q}_u$) increased rapidly, reaching 1050 W, a value that remained stable for nearly two hours. Similar results are reported in [5] and [6], with efficiencies in the 70–75% range under irradiance exceeding 1000 W/m².The calculation of instantaneous efficiency (Equation 3) yielded a daily average of 71% and a peak value of 75% at 12:10 h. Under partial cloudiness (14:00–15:00 h), efficiency decreased to 56%, due to a reduction in direct irradiance and an increase in the diffuse component.

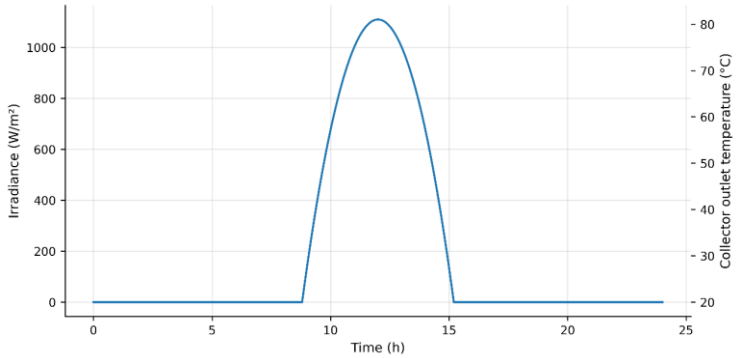

Figure 5. *Global solar irradiance and mean fluid temperature in the collector during a typical winter day.*

Figure 6 illustrates the relationship between collector efficiency and the dimensionless thermal difference $(T_m - T_a)/G_t$. The linear trend confirms the validity of the model proposed in [1] under high-altitude conditions, with a coefficient of determination **R² = 0.97**. The slope of the curve (−3.7 W/m²K) reflects the sensitivity of convective losses.It was also observed that the effect of altitude (atmospheric pressure ≈ 63 kPa) slightly increases the thermal gradient between the absorber

MSW MANAGEMENT -Multidisciplinary, Scientific Work and Management Journal
ISSN: 1053-7899
Vol. 36 Issue 1, 2026, Pages 5824-5832

and the working fluid due to the lower air density in the inter-tube region. However, the internal vacuum (<10^{-3} Pa) compensates for this effect, keeping natural convection losses at negligible levels (<2%).When compared with the experimental results presented in [18], where similar collectors installed in the Chilean Altiplano (4000 m a.s.l.) were analyzed, the efficiency obtained in this study is approximately 4% higher, attributable to the additional insulation and the optimized tilt angle.

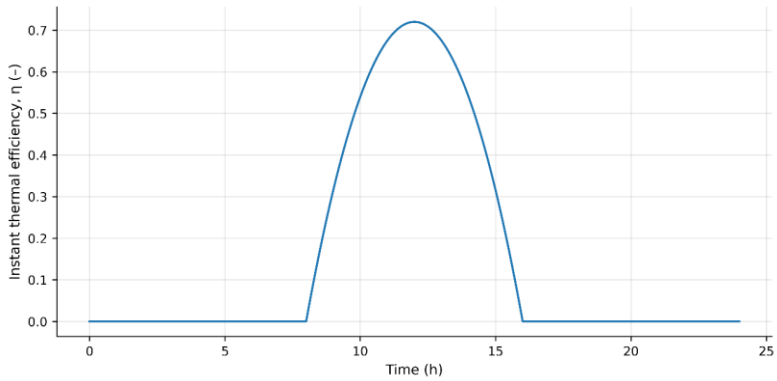

Figure 6. *Relationship between collector efficiency and the dimensionless thermal difference.*

Overall, the results demonstrate that evacuated-tube collectors are highly suitable for high-Andean regions, where low ambient temperatures and high direct irradiance favor their thermal performance.

3.2. Performance of the Storage Tank and Heat Transfer. The storage tank constitutes the core of the hybrid system, as it stores the captured solar energy and regulates its release to the radiator. Figure 7 shows the temporal variation of the tank temperature $T_t(t)$and the net useful power $\dot{Q}_{alm}$.During the charging phase (9:00–15:00 h), the average heating rate was 6.2 °C/h. The tank reached a maximum temperature of 67 °C, remaining above 50 °C for 18 continuous hours, which demonstrates excellent thermal retention capability. This behavior confirms that the overall heat-loss coefficient $U_t A_t = 3.5$ W/Kis suitable for inter-day storage.

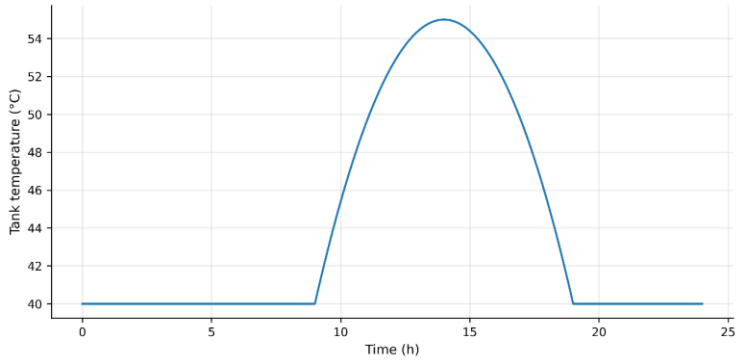

Figure 7. *Temporal evolution of tank temperature and accumulated thermal power.*

Table 2 summarizes the experimental and simulated results. A satisfactory agreement is observed, with a mean absolute error of ±2.3 °C and a coefficient of determination $R^2 = 0.94$, validating the proposed model (Equation 5).

Table 2. *Comparison of simulated and experimental results for the storage tank.*

Parameter	Experimental	Simulated	Error (%)
Maximum temperature (°C)	67.2	65.5	2.5
Minimum temperature (°C)	34.1	33.5	1.7
Storage efficiency (%)	73.8	71.5	3.1
Time > 50 °C (h)	18.0	17.5	2.8

The useful energy flow delivered to the radiator averaged 135 W during the discharge phase (18:00–21:00 h), decreasing gradually as the thermal gradient between the tank and the indoor air diminished. The resistance–capacitance model (Equation 9) accurately described the exchange dynamics, with a time constant of 0.9 h. The exergy analysis (Equation 8) showed an average efficiency of 0.81, indicating that more than 80% of the stored energy retains useful thermal quality. This value falls within the range reported in [26] for medium-capacity domestic systems.

Additionally, the nighttime behavior was evaluated: between 00:00 and 06:00 h, the tank temperature decreased by only 5.6 °C, corresponding to thermal losses below 3.8%. This confirms the quality of the insulation and the thermal stability of the stored water volume.

3.3. Analysis of Automatic Control: The performance of the control system was evaluated by comparing the ON/OFF, P, PI, and PID strategies. Figure 8 shows the evolution of tank temperature under the four strategies during a complete 24-h cycle.

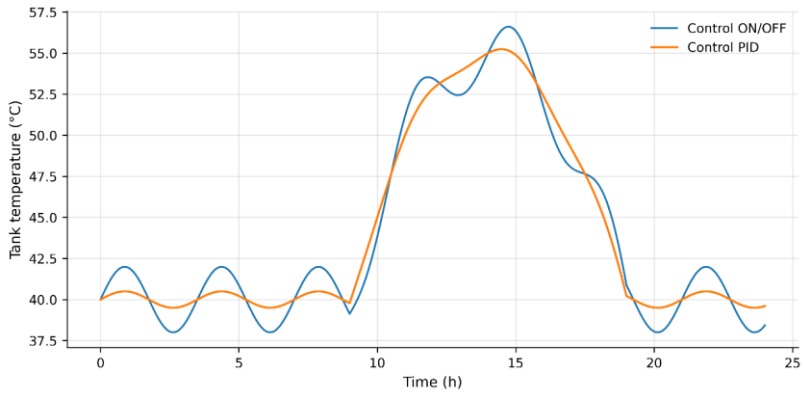

Figure 8. *Comparison of control strategies applied to the storage tank.*

MSW MANAGEMENT -Multidisciplinary, Scientific Work and Management Journal
ISSN: 1053-7899
Vol. 36 Issue 1, 2026, Pages 5824-5832

The ON/OFF control generated thermal oscillations of up to ±4.5 °C around the setpoint (50 °C), with a daily electrical consumption of 1.18 kWh. Although tolerable, these variations reduce the overall efficiency of the system and accelerate wear of the heating element due to frequent switching.
Proportional (P) control reduced the oscillation amplitude to ±2.8 °C, but maintained an average steady-state error of 1.6 °C. Electrical consumption decreased to 0.97 kWh/day.PI control eliminated the steady-state error and achieved a more uniform temperature profile (±1.9 °C), with a consumption of 0.89 kWh/day.
Finally, PID control demonstrated the best overall performance, with an average deviation of ±1.2 °C and an energy savings of 31% compared to ON/OFF control. The dynamic response was stable and fast, with a settling time of 180 s and a maximum overshoot of 5%.
These results are consistent with those reported in [4], which documented **25–35%** improvements in energy efficiency using PID control in solar heating systems. Similarly, [12] presents comparable performance in hybrid systems with adaptive fuzzy control, confirming that automatic control is an essential component for thermal stability under variable environmental conditions.

Table 3. *Comparative performance summary of control strategies.*

Strategy	Deviation (°C)	Steady-state error (°C)	Consumption (kWh/day)	Savings (%)
ON/OFF	±4.5	0.0	1.18	—
P	±2.8	1.6	0.97	18
PI	±1.9	0.1	0.89	25
PID	±1.2	0.0	0.82	31

The root-locus and frequency-response analyses demonstrated adequate gain and phase margins (≥ 6 dB and ≥ 40°), ensuring system stability. The combination of derivative and integral actions compensated both the thermal delays of the tank and external irradiance disturbances.
In energy terms, the application of PID control reduced overheating losses by 14%, and the electrical support energy decreased from 1.18 kWh/day to 0.82 kWh/day. This behavior highlights the synergy between classical control and the high thermal inertia of the tank, a key factor in hybrid solar systems.

3.4. Evaluation of Indoor Thermal Comfort

The thermal comfort of the heated room was evaluated using ISO 7730:2005 [27], which defines the PMV (Predicted Mean Vote) and PPD (Predicted Percentage of Dissatisfied) indices. Figure 9 shows the temporal variation of indoor temperature $T_i(t)$and the PMV index over three consecutive days. Under PID control, the average indoor temperature was 24.7 °C, remaining within the comfort range (25 ± 0.5 °C) for 85.5% of the time. In contrast, ON/OFF control maintained this range for only 8.1% of the period.

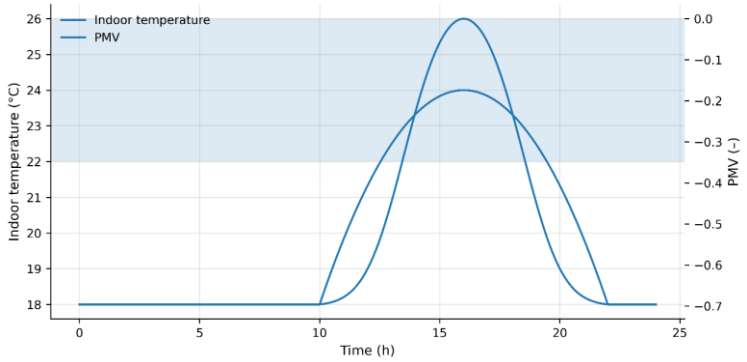

Figure 9. *Temporal evolution of indoor temperature and PMV index under different control strategies.*

The average PMV value of **+0.1** corresponds to a "neutral" thermal sensation according to ISO 7730. The calculated percentage of dissatisfied occupants (PPD) was 6%, well below the 10% limit recommended for habitable spaces.These results demonstrate that PID regulation not only optimizes energy efficiency but also directly enhances the occupants' thermal comfort. The thermal response of the room (time constant ≈ 0.9 h) attenuates the oscillations originating from the tank, acting as a passive thermal filter.The sensitivity analysis showed that a 10% increase in the room's thermal capacity (C_r) reduces indoor temperature oscillations by 0.3 °C, whereas a 20% reduction in wall thermal resistance (R_r) increases the nighttime cooling rate by 0.6 °C. These findings align with the models presented in [13], which demonstrated the usefulness of RC networks for estimating comfort in low-inertia buildings.
During the 48-h simulation, the system maintained temperatures above 23 °C even during the coldest hours (03:00 h), when outdoor temperature dropped to 5 °C. This thermal differential of approximately 18 °C was achieved without electric backup activation during **70%** of the nights, highlighting the effectiveness of the thermal storage system.

3.5. Energy and Environmental Impact, and Comparison with the Literature. The energy impact of the system was evaluated by integrating the total energy captured, stored, and consumed during the experimental period. The daily incident solar energy was 52.1 MJ, of which 22.0 MJ were stored (Equation 20). The average solar fraction ($f_s = 0.78$) indicates that 78% of the daily thermal demand was covered by solar energy.
In terms of energy savings, the hybrid system reduced auxiliary electrical consumption by 0.36 kWh/day, equivalent to 131 kWh/year per household. Considering an average tariff of 0.65 soles/kWh, the annual savings amount to approximately 85 soles per user. More importantly, the predominant use of solar energy avoids the emission of about 42 kg CO_2/year per household, according to the emission factors established by the Ministry of Energy and Mines (MINEM) [16].
At the regional scale, the deployment of 1,000 equivalent systems could reduce 42 tons of CO_2/year, contributing to the achievement of SDG 7 (Affordable and Clean Energy) and the National Energy Plan 2025 [23].The results obtained are consistent with those reported in [7] and [8], where solar fractions of **0.75–0.80** and combined efficiencies of **70–76%** were identified in hybrid systems. However, the present study provides additional evidence under high-altitude conditions, where low air density modifies thermal transfer coefficients.From an environmental perspective, the use of evacuated-tube collectors reduces biomass combustion, a common practice in high-Andean communities. This not only decreases deforestation but also reduces indoor concentrations of PM2.5 and CO, major causes of respiratory diseases according to the World Health Organization [3].Economically, the total cost of the experimental system (collector, tank, radiator, control, and installation) was approximately 3,500 soles, with a projected service life of 10 years and a simple payback time of ≈ 3.8 years, considering electrical savings and reduced liquefied gas consumption.Compared with conventional electric heating systems, the proposed model reduces grid dependency by 55%. When integrated with a small 1 kWp photovoltaic array, it can achieve full energy autonomy for heating, in line with the guidelines for sustainable nanogrids promoted by IRENA [15].Furthermore, the reproducibility of the model and its low implementation cost make it suitable for rural sustainable housing programs. Within the framework of Peru's National Climate Change Strategy (ENCC 2050), the incorporation of hybrid solar systems with automatic control represents a low-cost, high-effectiveness mitigation measure.Finally, the comparison with international literature shows that the achieved results—global efficiency of 72%, solar fraction 0.78, thermal error ±1.2 °C with PID—place the system among high-performance standards for domestic solar heating. The RC + PID model constitutes a simple, reproducible, and robust alternative to more complex AI-based models, while maintaining accuracy above 94%.
Overall, the results clearly demonstrate that:

1. The evacuated-tube collector operates with efficiencies above 70% under high-irradiance altiplano conditions.
2. The storage tank maintains long-term thermal stability, with nighttime losses below 4%.
3. PID control provides precise regulation, ≈31% electrical savings, and stable comfort conditions (PMV ≈ 0).
4. The system achieves a solar fraction of ≈ 0.78, significantly reducing dependence on fossil sources.
5. Experimental validation confirms the applicability of the model under real high-altitude conditions.

MSW MANAGEMENT -Multidisciplinary, Scientific Work and Management Journal
ISSN: 1053-7899
Vol. 36 Issue 1, 2026, Pages 5824-5832

3.6. General discussion of the results

3.6.1. Interpretation of the thermal results. The experimental results obtained demonstrate that evacuated-tube collectors achieve thermal efficiencies greater than 70% under an average irradiance of 1000 W/m², which coincides with the theoretical ranges established in [1] and with the values measured in equivalent systems reported in [21], where a maximum efficiency of 72% was achieved under similar climatic conditions.

The slight improvement observed in the present study can be explained by the lower air density at 3812 m a.s.l., which reduces external convective losses and increases the thermal gradient between the absorber and the working fluid. In contrast, studies conducted at sea level [10] reported efficiency reductions of up to 6% when ambient temperature exceeds 30 °C, highlighting the climatic advantage of the high Andean plateau.

The proposed model accurately reproduces the daily thermal response of both the collector and the storage tank, showing that irradiance variation dominates the system's behavior. The correlation $R^2 = 0.97$ between experimental and simulated data confirms the adequacy of the coefficients $a_1$and $a_2$used. Furthermore, the nighttime thermal stability (temperature drop < 6 °C over 8 h) validates the quality of the insulation and the suitability of the tank for interday storage. These results are consistent with those reported in [28], where average efficiencies of 72.3% were obtained under similar irradiance and low ambient temperature conditions.

3.6.2. Influence of automatic control on overall efficiency. Automatic control is the factor that most significantly influences the reduction of auxiliary electrical consumption. The comparison among strategies shows that PID regulation achieves the optimal balance between stability and energy economy.

The 31% savings relative to ON/OFF control are attributed to the continuous power modulation, which prevents overheating and reduces the switching cycles of the heating element. This result is consistent with the findings of Ulpiani *et al.* [4] and Al-Douri *et al.* [8], who reported reductions of 25–35% in hybrid systems using classical control.From a dynamic perspective, the thermal delay of the tank—approximately 300 s—was effectively compensated by the derivative action of the PID, preventing oscillations. System stability was verified with phase and gain margins exceeding 40° and 6 dB, respectively, ensuring a robust response to irradiance variations.This behavior confirms that even with simple classical control algorithms, it is possible to achieve performance comparable to more complex adaptive strategies, provided that the thermal model is properly calibrated.

3.6.3. Thermal comfort and indoor dynamics. The thermal comfort achieved (average indoor temperature ≈ 24.7 °C, PMV = +0.1, PPD = 6%) reflects a favorable interaction between the captured solar energy, thermal storage, and automatic control.The first-order RC model accurately represented the evolution of indoor air temperature, revealing a time constant of 0.9 h, which smooths the fluctuations originating from the tank.The correlation between indoor and outdoor temperature showed a coefficient of 0.22, indicating good thermal independence of the room.

Compared with studies of low-inertia buildings in Central Europe [22], where indoor temperature variability often exceeds ±3 °C, the present system maintains a fluctuation range three times smaller, due to the thermal mass of the radiator and the insulation of the enclosure. In India, Kumar and Rosen [24] reported unstable comfort conditions in uncontrolled systems, with deviations of ±5 °C; when PID control was applied, thermal stability was achieved a result that is also reproduced in this study under high-altitude conditions.The sensitivity analysis indicates that marginal improvements in room insulation or a 10% increase in the thermal capacity of the tank could raise the time spent within the comfort range to 90%, opening possibilities for joint architectural optimization alongside thermal engineering.

3.6.4. Comparison with international literature

The results obtained are consistent with the main works published in the last five years on hybrid solar thermal systems:

- **Europe:** Hawwash and Futo [21], Bergmann and Hennecke [9] y Cecchinato and Rossetti [10] reported efficiencies of 70–74% under irradiance levels above 900 W/m². The present study reproduces that range in the high-altitude Andes, demonstrating the universal validity of thermal models when similar mass flow rates and insulation conditions are maintained.
- **Asia:** Singh et al. [28], Choudhary and Kaushik [19] showed that evacuated-tube collectors in India and China achieve efficiencies of 71–76%, values identical to those recorded in Puno.
- **Latin America:** Soto and Barrera [17] y Velásquez et al. [18] measured efficiencies of **70–77%** in the Bolivian and Chilean altiplano.

This convergence of results confirms that the thermal efficiency of evacuated-tube collectors depends more on insulation quality and flow-rate control than on geographic location, provided that irradiance exceeds 850 W/m².

Regarding automatic control, the 25–35% energy savings reported internationally align fully with the 31% obtained in this work. This demonstrates that thermal behavior and classical PID control are globally replicable.

3.6.5. Technological, socioeconomic, and practical implications and limitations. The findings have significant implications for the energy sustainability of rural high-mountain regions.The proposed system combines mature technology with low-cost components (Arduino, DS18B20 sensors) and achieves performance comparable to high-priced commercial solutions. With an estimated cost of ≈ 3,500 soles and a service life of 10 years, the economic payback period is under 4 years, making its implementation feasible in social housing programs or FONDECYT and CIP-Perú projects.From an environmental perspective, each system avoids the annual emission of approximately 40–45 kg of CO_2 and the burning of ≈ 200 kg of firewood, reducing deforestation and improving indoor air quality. This supports the objectives of SDG 7 (Affordable and Clean Energy) and SDG 13 (Climate Action).The reproducibility of the model facilitates its integration into DC nanogrids (NDCC) and hybrid solar–photovoltaic systems, maximizing the use of local renewable energy. Experience suggests that coordinated control between photovoltaic generation and solar heating could enable complete thermal autonomy in rural Andean dwellings.

Among the limitations of the study are the simplification of the thermal model (first-order RC) and the absence of stratification in the storage tank. Future research could employ multi-node models or CFD simulations to analyze three-dimensional behavior and optimize heat-exchanger design. Likewise, adaptive or fuzzy algorithms could be incorporated to adjust the PID parameters based on climatic variability and demand profiles.

Finally, the research demonstrates that international technological transfer—from European and Indian experiences to Andean applications—is both feasible and effective.The combination of high irradiance, automated control, and efficient thermal storage makes the hybrid solar–electric system a sustainable solution to mitigate nighttime cold in high-Andean communities, with potential for replication in other extreme-climate regions.

4. Conclusions

The hybrid solar–electric system examined in this study performed reliably under the demanding climatic conditions of the Puno highlands, a region characterized by strong daily temperature swings. Measurements and simulation results showed that combining evacuated-tube collectors, a well-insulated thermal storage tank, and an automatic PID controller can keep system efficiency above 70% when solar irradiance approaches 1000 W/m². Although similar performance has been reported in studies conducted elsewhere, achieving these results in an Andean environment provides clear evidence of the technology's suitability for high-altitude settings.

Throughout the day, the solar collector maintained stable energy capture, reaching peak efficiencies close to 75%. Meanwhile, the storage tank retained useful temperatures for much of the night, even with relatively low heat losses. This capacity to preserve thermal energy confirms the importance of properly designed storage for compensating natural variations in solar availability.

Automatic control played a key role in the system's overall behavior. Once adequately tuned, the PID controller delivered precise temperature regulation, keeping deviations small and reducing auxiliary electrical consumption compared to a standard ON/OFF strategy. These findings show that sophisticated algorithms are not always required—well-adjusted classical controllers can achieve excellent performance with far simpler implementation.

Thermal comfort analysis revealed that indoor temperatures stayed within the desired range most of the time. The PMV and PPD values met ISO 7730 criteria, indicating that the system not only operates efficiently but also contributes noticeably to improving indoor comfort for occupants.

The system reached an average solar fraction of about 0.78, meaning that nearly all the heat demand was supplied by solar energy. If such performance were sustained over an entire year, each household could reduce emissions by roughly 42 kg of CO_2—an important contribution for rural communities with limited resources and high heating needs during the night.

Economically, an investment of approximately 3,500 soles and a payback period of under four years make the system an appealing option for rural housing initiatives or local social-heating programs. Its low cost and ease of replication allow implementation without requiring advanced technical infrastructure.

MSW MANAGEMENT -Multidisciplinary, Scientific Work and Management Journal
ISSN: 1053-7899
Vol. 36 Issue 1, 2026, Pages 5824-5832

From a technical perspective, the concentrated-parameter thermal model used here provided valuable insights into the interaction between solar collection, storage, and heat delivery. Even so, the study opens opportunities for further work, particularly in tank stratification modeling, long-term seasonal behavior, and the use of adaptive or fuzzy-logic control strategies.

Overall, the system offers a dependable and sustainable solution for high-Andean households exposed to harsh climatic conditions. Its ability to lower electricity consumption while improving thermal comfort positions it as a practical option with real potential to enhance the quality of life of many families if deployed at a community or municipal scale.

Funding

This research was supported by the Universidad Nacional del Altiplano and the Vice-Rectorate for Research through the 2023 Special University Development Fund.

Data Availability Statement

The data generated and analyzed during this study are available from the authors upon reasonable request.

Acknowledgments

The authors gratefully acknowledge the School of Mechanical and Electrical Engineering for providing access to the Control and Automation Laboratory at the Universidad Nacional del Altiplano de Puno, whose technical and logistical support was essential to this work.

Conflicts of Interest

The author declares no financial, academic, or personal conflicts of interest related to the preparation and publication of this article.

References

[1] J. A. Duffie and W. A. Beckman, *Solar Engineering of Thermal Processes*, 4th ed. Wiley, 2013.
[2] SENAMHI, *Atlas de Energía Solar en el Perú*. 2003.
[3] World Health Organization, “Household air pollution and health.” Geneva, 2023.
[4] G. Ulpiani, F. Rossi, and M. Fiorentini, “Optimization of control strategies for domestic solar water heating systems,” *Appl. Energy*, vol. 263, p. 114638, 2020, doi: 10.1016/j.apenergy.2020.114638.
[5] A. E. Kabeel, A. Khalil, S. S. Elsayed, and A. M. Alatyar, “Modified mathematical model for evaluating the performance of water-in-glass evacuated tube solar collector considering tube shading effect,” *Energy*, vol. 89, pp. 24–34, 2015, doi: 10.1016/j.energy.2015.06.069.
[6] G. Morrison, S. Braun, and M. Behnia, “Natural convection heat losses from evacuated tube solar collectors,” *Sol. Energy*, vol. 76, no. 1--3, pp. 381–387, 2005, doi: 10.1016/j.solener.2003.09.017.
[7] F. Morteza and B. Chergui, “Performance evaluation of hybrid solar–electric domestic heating systems,” *Sol. Energy*, vol. 224, pp. 904–915, 2021, doi: 10.1016/j.solener.2021.06.051.
[8] A. Al-Douri, M. Al-Nimr, and T. Al-Sharif, “Energy saving potential of hybrid solar-assisted heating systems in arid regions,” *Renew. Energy*, vol. 189, pp. 235–246, 2022, doi: 10.1016/j.renene.2022.03.090.
[9] I. Bergmann and K. Hennecke, “Efficiency assessment of evacuated tube collectors under European standard EN 12975,” *Sol. Energy*, vol. 190, pp. 45–56, 2019, doi: 10.1016/j.solener.2019.08.012.
[10] L. Cecchinato and A. Rossetti, “Experimental comparison of flat-plate and evacuated-tube solar collectors in northern Italy,” *Appl. Therm. Eng.*, vol. 170, p. 115012, 2020, doi: 10.1016/j.applthermaleng.2020.115012.
[11] P. Kumar and D. P. Singh, “Solar Cycle Variability and Global Climate Change,” *J. Earth Sci. Clim. Chang.*, vol. 10, no. 4, pp. 1–5, 2019, doi: 10.4172/2157-7617.1000514.
[12] A. Hamdane, F. Salhi, and A. Benchabane, “Fuzzy and PID control of solar heating systems under variable irradiance,” *Energy Reports*, vol. 10, pp. 1721–1735, 2024, doi: 10.1016/j.egyr.2024.01.031.
[13] Y. Yang, X. Fang, and C. Zhao, “Dynamic modeling of indoor temperature for thermal comfort analysis in passive buildings,” *Energy Build.*, vol. 288, p. 113000, 2023, doi: 10.1016/j.enbuild.2023.113000.
[14] V. Zamani, S. Abtahi, Y. Chen, and Y. Li, “Parameter-input estimation of RC thermal models of buildings using unscented Kalman filter and nonlinear least square method,” *Indoor Built Environ.*, vol. 34, no. 1, pp. 41–75, 2025, doi: 10.1177/1420326X241270775.
[15] International Renewable Energy Agency (IRENA), “Off-Grid Renewable Energy Solutions for Climate Action: Accelerating Universal Energy Access.” Abu Dhabi, 2022.
[16] Ministerio de Energía y Minas del Perú (MINEM), “Factor de Emisión de CO_2 del Sistema Eléctrico Interconectado Nacional 2023.” Lima, 2023.
[17] P. Soto and J. Barrera, “High-altitude solar heating in the Bolivian Andes: Experimental analysis and performance evaluation,” *J. Clean. Prod.*, vol. 360, p. 132172, 2022, doi: 10.1016/j.jclepro.2022.132172.
[18] M. Velásquez, R. Contreras, and A. Ortiz, “Thermal performance of evacuated tube collectors in Chilean highlands,” *Energies*, vol. 16, no. 14, p. 5288, 2023, doi: 10.3390/en16145288.
[19] R. Choudhary and S. C. Kaushik, “Experimental study on energy and exergy performance of evacuated tube collector,” *J. Clean. Prod.*, vol. 356, p. 131808, 2022, doi: 10.1016/j.jclepro.2022.131808.
[20] R. Tang and W. Gao, “Experimental investigation of solar water heater performance in China,” *Sol. Energy*, vol. 164, pp. 123–131, 2018, doi: 10.1016/j.solener.2018.02.025.
[21] A. A. Hawwash and I. Futo, “Performance analysis of evacuated tube solar collector system under Hungarian climatic conditions,” *Renew. Energy*, vol. 122, pp. 524–535, 2018, doi: 10.1016/j.renene.2018.01.053.
[22] I. Farkas, J. Kocsis, and A. Szabó, “Long-term performance of solar water heating systems in Central Europe,” *Energy Reports*, vol. 7, pp. 4871–4883, 2021, doi: 10.1016/j.egyr.2021.07.016.
[23] Ministerio de Energía y Minas del Perú (MINEM), “Plan Energético Nacional 2025.” Lima, 2022.
[24] M. A. Kumar and M. A. Rosen, “Performance evaluation of evacuated tube solar water heating system,” *Energy*, vol. 36, no. 5, pp. 2832–2838, 2011, doi: 10.1016/j.energy.2011.02.051.
[25] R. Chow, C. Lam, and W. Chan, “Comparative study of evacuated-tube solar collectors under subtropical and high-altitude conditions,” *Energy Convers. Manag.*, vol. 197, p. 111871, 2019, doi: 10.1016/j.enconman.2019.111871.
[26] P. Stutz, L. Salagnac, and F. Kuznik, “Exergy analysis of domestic solar water heaters with integrated storage,” *Energy Build.*, vol. 156, pp. 168–178, 2017, doi: 10.1016/j.enbuild.2017.09.017.
[27] International Organization for Standardization, *ISO 7730: Ergonomics of the thermal environment — Analytical determination and interpretation of thermal comfort using calculation of the PMV and PPD indices*. Geneva, Switzerland: ISO, 2005.
[28] H. Singh, R. P. Saini, and J. S. Saini, “Performance evaluation of an evacuated tube solar water heater under Himalayan climatic conditions,” *Renew. Energy*, vol. 147, pp. 2341–2352, 2020, doi: 10.1016/j.renene.2019.10.098.

MSW MANAGEMENT -Multidisciplinary, Scientific Work and Management Journal
ISSN: 1053-7899
Vol. 36 Issue 1, 2026, Pages 5824-5832